



AI and Machine Learning for Breast Cancer Diagnosis Using Histopathology and Clinical Decision Systems

Swati R. Nitnaware^{1,*}, Bindu Madhavi Tummala², Naga Siva Jyothi Kompalli³, Lakshmi Ramani Burra⁴, Nelli Sreevidya⁵, Gunavardini V.⁶

¹Asst. Professor, Dept. of Electronics Engineering, Yeshwantrao Chavan College of Engineering, Nagpur, Maharashtra, India

²Assistant Professor, Department of CSE, Velagapudi Ramakrishna Siddhartha School of Engineering, Siddhartha Academy of Higher Education (Deemed to be University) Vijayawada, AP, India

³Associate Professor, Dept. of CSE, Sreenidhi Institute of Science and Technology, Hyderabad, Telangana, India

⁴Associate Professor, Dept. of CSE, Koneru Lakshmaiah Education Foundation, Vaddeswaram AP, India

⁵Assistant Professor, Department of IT, Sreenidhi Institute of Science and Technology, Hyderabad, Telangana, India

⁶Assistant Professor, Department of CSE, Bannari Amman Institute of Technology (Autonomous), Sathyamangalam, Erode, TN, India

Emails: swatitidke02@gmail.com; bindumadhavi@vrsiddhartha.ac.in; sivajyothi.p@sreenidhi.edu.in; ramanimythili@gmail.com; sreevidya.n@sreenidhi.edu.in; gunavardini@bitsathy.ac.in

Abstract

The diagnosis of breast cancer depends on histopathology for precise and trusted evaluation between malignant tumor cells and benign cells. The analysis demands significant time and creates additional room for human errors. A deep learning approach for computer-aided diagnosis (CAD) establishes techniques to enhance the classification performance in this study. The proposed methods utilize One-hot encoding with VGG-16 for feature extraction to achieve 98% accuracy with BreakHis data while DBN for feature learning reaches 98% accuracy on BreakHis and 96% on Kaggle. SSGAN addresses unannotated images effectively with up to 89% accuracy. Through its application, deep learning technology proves to enhance breast cancer identification while decreasing the workload on medical pathologists. One-hot encoding remains efficient for computations yet the DBN extraction method produces superior features. The SSGAN model increases labeling accuracy when it uses available labeled data and unlabeled data to lower annotation expenses. Deep learning technologies validate their ability to transform breast cancer histopathological diagnosis through precision-enhanced efficient examination methods especially with semi-supervised GAN systems.

Received: December 31, 2024 Revised: February 25, 2025 Accepted: March 31, 2025

Keywords: Breast Cancer Diagnosis; Deep Learning; Computer-Aided Diagnosis (CAD); CNNs; Deep Belief Network (DBN); Semi-Supervised Generative Adversarial Network; Medical Image Analysis; Machine Learning in Healthcare; Tumor Classification

1. Introduction

Artificial intelligence technology enhances breast cancer diagnosis through better results with complex imaging systems. AI technologies support mammography screening as the primary method by addressing issues that produce false positive results. Thermography needs better development because it shows sensitivity to environmental fluctuations. Research indicates that sonography achieves high accuracy rates through its combination with CNN architectures [1]. The combination of histopathology testing together with AI models

gives practitioners near-perfect diagnostic capabilities. Future investigations need to boost the general applicability of datasets and cut down calculations expenses and establish AI systems that handle and analyse various imaging inputs to enhance clinical diagnosis capabilities.

Histopathological analysis represents the standard method for diagnosing breast cancer because it delivers vital information about breast tissue microstructure. The standard histopathological assessment process works slowly and needs skilled pathologists along with suffering from differences between pathologists [2]. Breast cancer diagnosis requires modern computational approaches because its complex variants together with expanding diagnostic activity require better diagnostic results and operational efficiency. Figure 1 illustrates the stages that can be segregated in breast cancer.

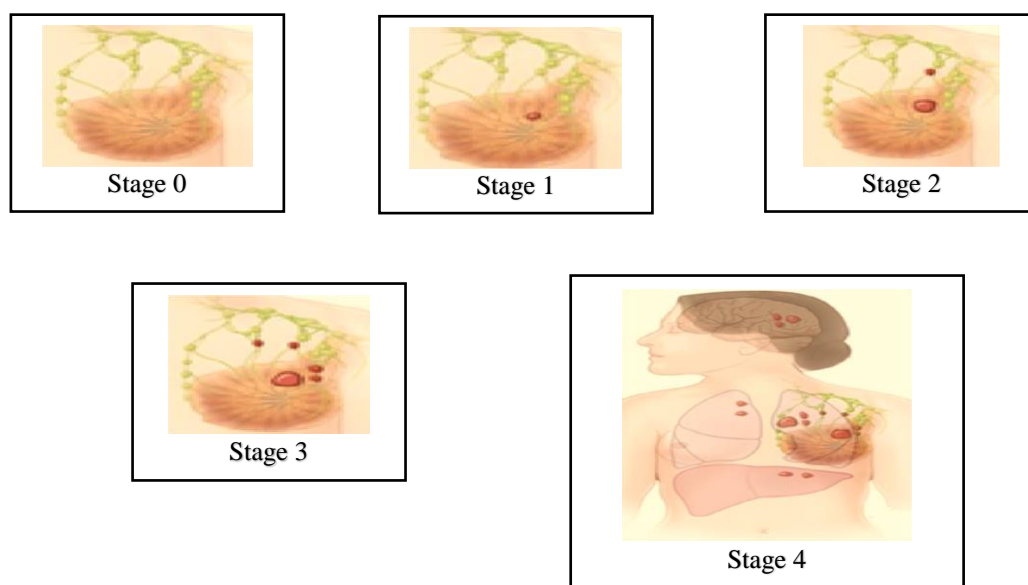


Figure 1. Stages of Breast cancer

The medical field has experienced a transformation through artificial intelligence (AI) which has specifically revolutionized cancer diagnostic analysis since the past few years. The detection process of breast cancer as well as its classification benefit remarkably from artificial intelligence techniques that combine machine learning (ML) and deep learning (DL) [3]. AI technology applied to diagnostic images of histopathology improves healthcare results through three key benefits: it reduces mistakes made by humans and establishes standardized reading methods while speeding up the diagnosis of malignant cell identification.

AI creates powerful opportunities for breast cancer diagnosis through Clinical Decision Support Systems, which lead to highly promising advancements. Pathologists receive AI-based assistance to diagnose breast cancer through the analysis of histopathological images, which delivers both accurate and uniform diagnostic results [4]. Medical staff who implement AI-driven CDSS into their clinical operations will boost diagnostic speed and lessen their work duties that leads to better patient recovery results.

Breast cancer exists as a heterogeneous disease, which takes four main forms: invasive ductal carcinoma along with invasive lobular carcinoma in addition to ductal carcinoma in situ and triple-negative breast cancer. The right classification of these subtypes requires accurate identification for selecting proper therapeutic methods. The diagnostics field depends on current methods that use radiological techniques including mammography together with ultrasonography and magnetic resonance imaging (MRI) [5]. The diagnostic techniques render effective results yet come with known performance constraints of artificially stimulated readings versus inaccurate determination together with the difficulty to separate benign and malignant tissue types. Artificial intelligence analysis of histopathological samples creates a more specific and fact-based method for improving existing diagnostic limitations.

Medical pathology uses digital images joined with AI pattern recognition to achieve groundbreaking efficiency in its operations. Through whole slide, imaging (WSI) doctors can digitize their histopathological slides, which AI algorithms can process effectively on large datasets that show high accuracy. Extensive training of AI models enables them to spot complex morphological features which human pathologists find difficult to observe [6].

New diagnostic possibilities emerge because of the technological advances that provide more consistent, flexible, and large-scale diagnostic systems. Figure 2 shows the different approach of image scanning of breast cancer.

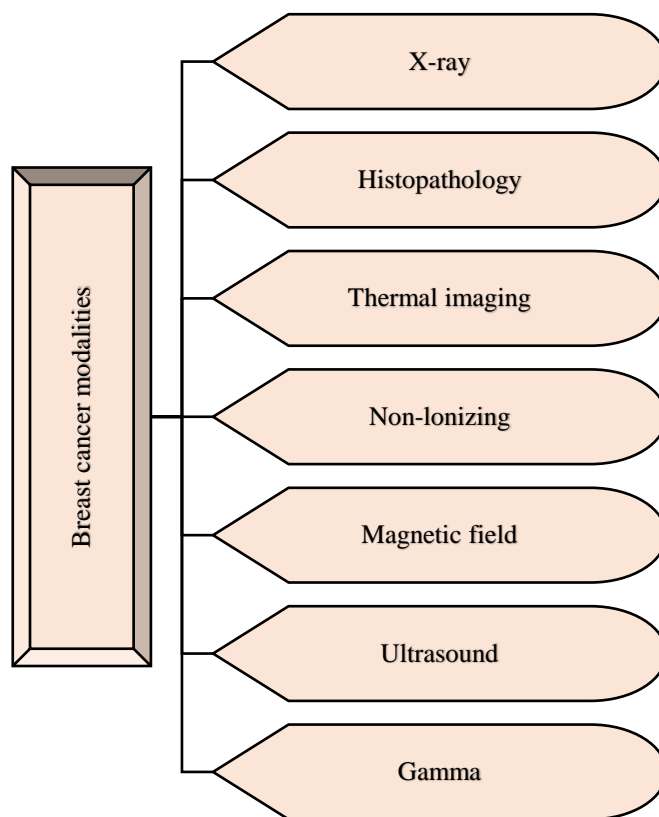


Figure 2. Diagnostic methods of Breast cancer

Convolutional neural networks (CNNs) within deep learning bring exceptional results in medical image examination. The hierarchical features extracted through CNN-based models allow automatic identification of normal tissue from cancerous tissues in histopathological images. Pre-trained models can handle specific diagnostic tasks when transfer techniques apply which lowers the requirement for extensive labelling of datasets [7]. When AI models join forces with traditional image processing methods people can enhance both feature extraction quality as well as accuracy levels.

Several obstacles continue to impede the advancement of AI-based breast cancer diagnostic systems after their notable achievements. The fundamental challenge exists in obtaining numerous top-quality labelled datasets needed to train AI detection algorithms. The quality variations present in histopathological images combined with staining procedures and scanner settings reduce model performance levels [8]. AI models need thorough interpretation and explanation capabilities in order to be accepted both from medical practitioners as well as from regulatory organizations. The successful adoption of AI technologies in clinical practice demands research communities to team up with pathologists and AI developers for developing seamless integration solutions.

Artificial intelligence goes further than histopathology diagnosis by incorporating other breast screening methods including mammography and thermography and sonography examinations. Medical experts have utilized AI algorithms to analyse mammograms along with the detection of microcalcifications and examination of breast densities. Medical practitioners use thermography to detect breast tissue temperature variations without invasive procedures for breast cancer detection [9]. The utilization of AI for thermographic analysis enables the detection of minimal temperature irregularities linked to malignancy conditions, which enhances examination performance. AI-based ultrasound imaging technologies help medical professionals correctly identify benign breast lesions from malignant ones thus cutting down the number of unnecessary biopsy procedures.

The merger of artificial intelligence with breast cancer diagnosis will redefine both patient-specific medical treatments and specific oncology applications. Predictive AI models help medical systems evaluate treatment hazards for single patients to create personalized care procedures. Through integrating AI with CDSS, medical

professionals obtain real-time help in oncology treatment decisions that leads to evidence-based clinical choices [10]. The monitoring of treatment response as well as recurrence detection that AI performs results in enhanced patient wellness throughout the long term.

This paper follows a structured format that begins with Section 2 which reviews previously conducted studies on AI approaches for breast cancer detection in multiple imaging types. The study objectives along with diagnostic accuracy improvement requirements through deep learning are detailed in Sections 3 and 4. The section details the dataset information with an explanation of the research experimental design in Sections 5 and 6. Section 7 demonstrates the methodology by selecting a dataset for preprocessing alongside proposing a VGG-16 along with DBN and SSGAN based deep learning system. This part describes the experimental design and evaluation methodology along with performance evaluation measures for the models along with their resulting data and method-performance comparison to current approaches. The study ends through Section 9, which provides both a summary of main findings and prospective directions for future research investigations.

2. Related Work

The use of Artificial Intelligence (AI) helps detect breast cancer early, which subsequently decreases mortality statistics through better diagnostic accuracy and therapeutic methods. Medical science has created multiple breast cancer detection tools that include mammography and thermography and sonography and histopathology imaging methods [11]. The precise diagnosis and automated image understanding through machine learning and deep learning represent two key artificial intelligence technologies that enhanced the quality of these cameras.

2.1 Mammography

Current medical practice uses Mammography as the main diagnostic imaging method for breast cancer because it produces X-ray images with low exposure rates. Modern mammogram evaluation uses radiologists as traditional diagnostic methods however, AI enhances detection results. The combination of SVM and Decision Trees with CNN and other DL models serves as data processing tools for breast cancer detection [12]. The detection methods of mammography face challenges when dealing with breast tissue density while still producing incorrect positive results.

2.2 Thermography

Breast cancer detection through thermography depends on monitoring temperature differences throughout breast tissues. The way malignant tumors affect blood circulation causes them to show distinct temperature patterns. The differentiation of benign from malignant lesions relies on the capabilities of Adaboost and SVM as part of AI-based classifier systems [13]. The accuracy of thermography testing is presently restricted since it responds to changes in environmental elements.

2.3 Sonography

The diagnostic technique of ultrasound examination functions well to detect solid tumors alongside distinguishing cysts. The implementation of CNN-based architectures by AI led to better medical diagnosis outcomes [14]. The application of traditional ML classifiers Random Forest and K-Nearest Neighbours (KNN) used to exist however, DL models ResNet and VGG bring much better detection accuracy.

2.4 Histopathology

The high-resolution imaging of breast tissue through histopathology analysis makes it the accepted method to confirm cancer cases. AI methods employ DenseNet and AlexNet with other DL architectures to achieve better tumour classification results. SSGAN represents a model that achieves commendable outcomes from training using scarce-labelled data [15].

Table 1: Literature survey on AI techniques used for breast cancer detection across different imaging modalities.

Imaging Modality	AI Technique Used	Feature Extraction Method	Dataset Used	Limitations
Mammography	CNN, SVM, PCA, Transfer Learning [16]	Histogram of Oriented Gradients (HOG), Gray Level Co-occurrence Matrix (GLCM), Principal Component Analysis (PCA)	MIAS, DDSM, INBreast	Fails in dense breast tissue, High false positives/negatives
Thermography	Adaboost, SVM, Curvelet Transform	Wavelet Transform, Curvelet Transform, Statistical [17] Features	Private Datasets	Sensitive to environmental temperature, Lower resolution images
Sonography (Ultrasound)	CNN (ResNet, VGG), Random Forest, KNN	Anisotropic Diffusion Filtering, Texture Analysis, Radiomics Features	Mendeley Repository, Private Datasets	Operator-dependent image quality, Presence of speckle noise [18]
Histopathology	DenseNet, AlexNet, SSGAN, Deep Belief Networks (DBN)	Color Normalization, Stain Augmentation, Patch-based Feature Extraction [19]	BreakHis, Kaggle	Requires biopsy, Expensive and time-consuming process
Magnetic Resonance Imaging (MRI)	Deep CNN, Random Forest, Autoencoders	Intensity Normalization, Fourier Transform, Region-based Analysis	Breast MRI Datasets (TCGA, RIDER)	Expensive, Long scanning time, Claustrophobia issues [20]
Positron Emission Tomography (PET)	CNN, Hybrid AI Models (ML + DL)	SUV-based Feature Extraction, Radiomics Features [21]	Public PET Imaging Databases	Exposure to radiation, High cost, Limited availability
Computed Tomography (CT)	Deep Learning (3D-CNN), Gradient Boosting	3D Feature Extraction, Edge Detection, Texture Features	LIDC-IDRI, Private Datasets [22]	High radiation dose, not ideal for frequent screening

The introduction of artificial intelligence enhances breast cancer diagnosis achievements by handling complicated imaging setups [23-25]. AI technologies support mammography screening as the primary method by addressing issues that produce false positive results. Thermography needs better development because it shows sensitivity to environmental fluctuations [26-28]. Research indicates that sonography achieves high accuracy rates through its combination with CNN architectures. The combination of histopathology testing together with AI models gives practitioners near-perfect diagnostic capabilities. Future investigations need to boost the general applicability of datasets and cut down calculations expenses and establish AI systems that handle and analyse various imaging inputs to enhance clinical diagnosis capabilities [29-30].

3. Objective of the Research

The main goal of this investigation is to improve breast cancer diagnosis precision and speed through advanced deep learning methods that process histopathology image data. The study aims to:

- ❖ The project needs to develop deep learning models, which will improve diagnostic accuracy and efficiency for breast cancer through histopathology image examinations.

- ❖ The investigation will identify one-hot encoding VGG-16 along with Deep Belief Networks and Semi-Supervised Generative Adversarial Networks as the most optimal classification scheme.
- ❖ Deep learning techniques should be implemented to enhance automatic pattern detection in histopathology images so features and classifications improve with decreased human involvement.
- ❖ SSGAN semi-supervised learning techniques provide efficient data utilization between labelled and unlabelled data for minimizing annotation expenses while preserving diagnostic achievement.

The objectives serve to advance medical imaging through AI while improving clinical results and assisting early cancer detection operations.

4. Motivation

Breast cancer stands as a major reason for female mortality across the world because prompt and exact diagnosis creates better prospects for successful treatment and enhanced survival outcomes. The gold standard for breast cancer diagnosis depends on histopathology though tissue examination by hand demands significant time while only experts can analyse the samples without errors. Standard machine learning techniques use manually designed features because they prevent system flexibility when working with different data pools.

CNNs and GANs used as part of deep learning analysis have achieved solid success in automating medical image analysis while producing precise outcomes. The current implementations face difficulties related to requiring extensive labelled datasets and tumour identification accuracy as well as operational speed limitations. The goal behind this research is to build reliable deep learning models that boost medical diagnoses while minimizing pathologist workload under a framework utilizing labelled and unlabelled data to optimize breast cancer detection scales.

5. Dataset

The authors utilize the major histopathology datasets BreakHis and Kaggle's Breast Cancer Histopathology to train deep learning models for obtaining breast cancer classifications. High-resolution breast tissue samples stored in these two datasets are divided into benign and malignant categories to service model training objectives.

The BreakHis dataset contains histopathological images from breast biopsy samples shown at microscopic levels ranging from 40× to 100× to 200× and 400×. The different magnification levels in the data enable models to learn from many visual attributes, which improves their ability to generalize. The dataset contains two tumour categories which are the benign section containing Adenosis and Fibroadenoma and Tubular Adenoma and Phyllodes Tumor and the malignant division that includes Ductal Carcinoma and Lobular Carcinoma and Mucinous Carcinoma and Papillary Carcinoma. This vast dataset provides critical value to deep learning model training because it contains numerous breast tumour types for discrimination.

The Kaggle Breast Cancer Histopathology dataset centres on studying Invasive Ductal Carcinoma (IDC) because it represents one of the most frequent and dangerous types of breast cancer. The data collection contains biopsy images that are tagged either as malignant IDC-positive or as benign IDC-negative samples. The dataset functions as a significant resource for binary classification tasks even though it lacks the multi-magnification feature found in BreakHis.

The preprocessing workflow applied to the dataset allowed for improvement of model accuracy and provided consistency. The input dimensions needed for deep learning required standardization through image resizing procedures. A colour normalization process neutralized inconsistent staining procedures to prevent their introduction of irregularities within histopathological images. Artificial expansion of the dataset through data augmentation techniques like rotation among others combined with flipping and contrast enhancement and noise addition reduced overfitting and enhanced the model robustness.

The research adopts these datasets to properly assess multiple deep learning approaches as it builds dependable and effective detection models for breast cancer.

6. Experimental Set Up

The research employed deep learning algorithms and trained them for breast cancer assessment through the analysis of histopathology pictures. The researchers used Python together with Keras and TensorFlow frameworks for implementing their experiments. A powerful GPU accelerated the training routines for complex deep neural network processes.

Progressive image pre-processing involved converting BreakHis dataset images and Kaggle dataset images to 224×224×3 pixels right before training began. This ensured compatibility with deep learning architectures. The model's robustness and overfitting prevention were accomplished through the application of data augmentation techniques that included rotation and flipping besides contrast adjustments. The data split into 80% training data and 20% validation data occurred through random selection.

A deep learning workflow used three methods including VGG-16 as a transfer-learning tool combined with DBN features extraction and SSGAN for integrating labelled and unlabelled data processing. Adam optimizer operated with 0.0001 learning rate and batch sizes of 100 to train every model. Multiple training epochs occurred but included early stopping controls to prevent overfitting from happening. Several rounds of model optimization took place through both the modification of hyperparameters and the optimization of network layers.

7. Proposed Work

Breast cancer stands as one of the widespread cancer types globally and thus needs both prompt diagnoses along with precise detection to deliver successful treatment outcomes. A pathologist performs tissue examination to diagnose breast cancer yet this method consumes time while presenting subjective reading challenges. Deep learning approaches now assist in automated histopathology image analysis because experts need help classifying images as benign or malignant. Current traditional machine learning techniques experience considerable difficulties in the analysis of complex histopathology images because they have problems with feature extraction while needing high levels of annotation and achieving accurate classification methods. Figure 3 shows the overview of the suggested approach.

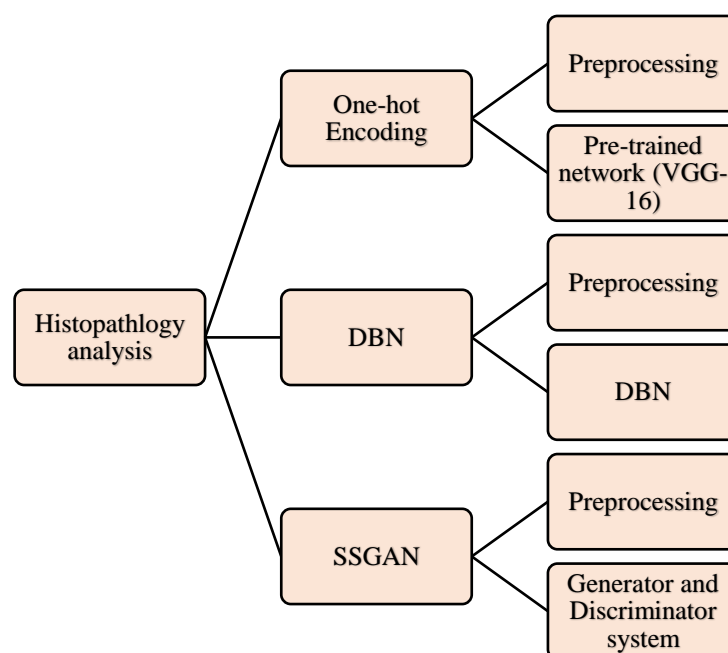


Figure 3. Illustrating the overview of suggested approach

This research work develops a comprehensive solution through the combination of three deep learning methodologies.

- ❖ The study implements VGG-16 as its pre-trained convolutional neural network (CNN) to perform breast cancer classification after additional fine-tuning.
- ❖ DBN uses RBMs arranged in multiple layers as an unsupervised feature learning approach before performing supervised classification tasks.
- ❖ The classification method SSGAN combines both supervised and unsupervised learning techniques to obtain better results and lower annotation expenses.

The proposed method integrates these three methods to produce reliable feature extraction while ensuring that classification runs smoothly along with extensive processing capacity for large histopathology datasets that needs minimal user involvement.

7.1 Preprocessing and Data Augmentation

A standard preprocessing protocol must run on histopathology images to achieve data consistency among different datasets before deep learning model application. Deep learning models experience inferior performance when working with biopsy sample images that differ in dimensions as well as color distribution and magnification degrees. Multiple preprocessing measures such as image resizing and normalization with augmentation are performed to manage these problems.

A standard image dimension is achieved through resizing which CNN-based models require for their inputs. The VGG-16 model requires $224 \times 224 \times 3$ pixels for input and therefore the images receive this standardized dimensional format. The model benefits from standard-sized data since it enables structured learning that reduces complexity and strengthens accuracy results.

During model training normalization functions to normalize pixel values to stabilize numerical computation. The wide pixel value scale from 0 to 255 within deep learning causes unstable gradients which results in inefficient learning processes. The normalization process includes scaling pixel values between $[0,1]$ by using min-max normalization which applies this equation:

$$A' = \frac{A - A_{min}}{A_{max} - A_{min}} \quad (1)$$

Where A = original pixel, A' = normalized image, A_{min} = minimum pixel value, A_{max} = maximum pixel values.

The training process requires data augmentation as an important method to achieve model generalization and reduce overfitting whenever datasets remain relatively small. The augmentation process expands training data through various changes including rotation and flipping together with brightness modifications and contrast adjustment and Gaussian noise application. Through such transformations, the model becomes more skilled at identifying common features across histopathology images thereby gaining resistance to image variations.

Image rotation produces random angular displacements from 0° to 180° to prevent the model from depending on tissue structure orientation. During flipping operations, the model applies front-to-back flips and side-to-side flips to generate alternative tissue view assessments. The visibility of cells becomes clearer through contrast adjustments which results in more accurate classification of specimens. Pixel values benefit from Gaussian noise addition because it creates small variations, which promote model performance on previously unseen data.

The dataset is split randomly into training at 80% and validation at 20% for proper model assessment.

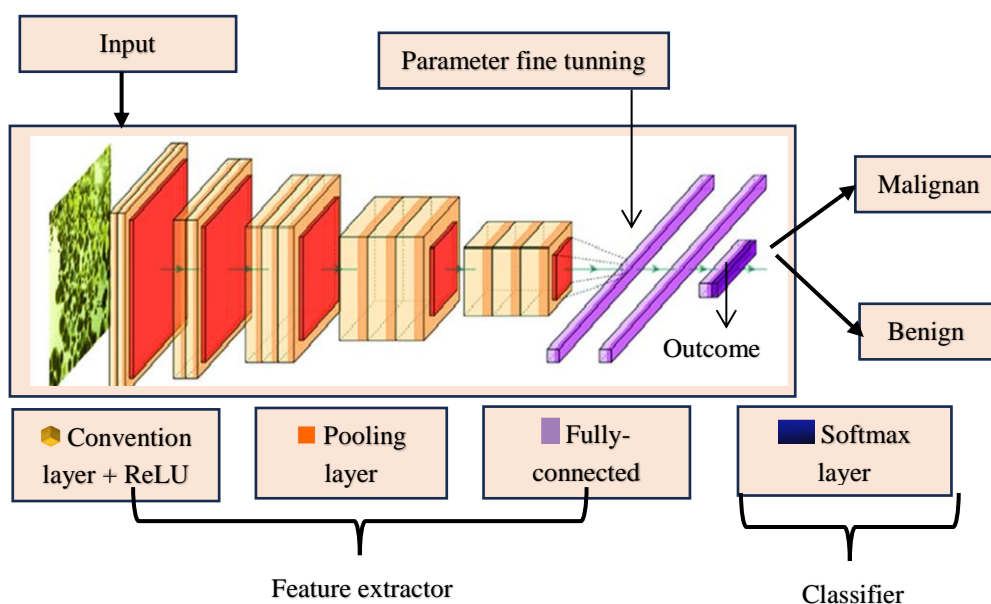


Figure 4. Classification based on transfer learning using VGG-16

7.2 Transfer Learning with VGG-16 for Breast Cancer Classification

Deep learning systems need substantial data labeling amounts to reach optimal performance rates. Acquiring large annotated medical image datasets remains challenging since pathologists need to perform manual sample labeling as an expert requirement. The solution to this data scarcity lies in transfer learning that takes a pre-trained ImageNet model to adapt it for another but related imaging task.

The researchers select VGG-16 as their model for transfer learning purposes as shown in Figure 4. The deep convolutional neural network VGG-16 consists of 16 layers, which contain convolutional pools and fully connected mathematical layers. The foundation of VGG-16 stays intact to detect generic image features including edges along with textures and shapes while its fully connected layers have been restructured to perform benign or malignant classification of breast cancer images.

The convolutional layers in VGG-16 generate various hierarchical features that exist within input image X. The set of filters W functions during convolutional operations for spatial pattern detection in the image.

$$A' = f(W * A + b) \quad (2)$$

$$f(a) = \max(0, a) \quad (3)$$

Assigning probability for every class, the function of softmax activation performs the final categorization:

$$P(y = j|A) = \frac{e^{W_j^T X + b_j}}{\sum_{k=1}^K e^{W_k^T X + b_k}} \quad (4)$$

With the category cross-entropy loss function as its basis, the framework is trained:

$$L = -\sum_{i=1}^N y_i \log \hat{y}_i \quad (5)$$

The model makes frequent weight updates through the Adam optimizer according to the following process:

$$W_{t+1} = W_t - \eta \frac{m_t}{\sqrt{v_t + \epsilon}} \quad (6)$$

Where A' = feature map after convolution, W = kernel weight, $*$ = convolution operation, b = bias term, $f(x)$ = ReLU activation function, K = nu of outcome classes, y_i = true label, \hat{y}_i = predicted probability, η = learning rate, m_t = first moment estimates, v_t = second moment estimates.

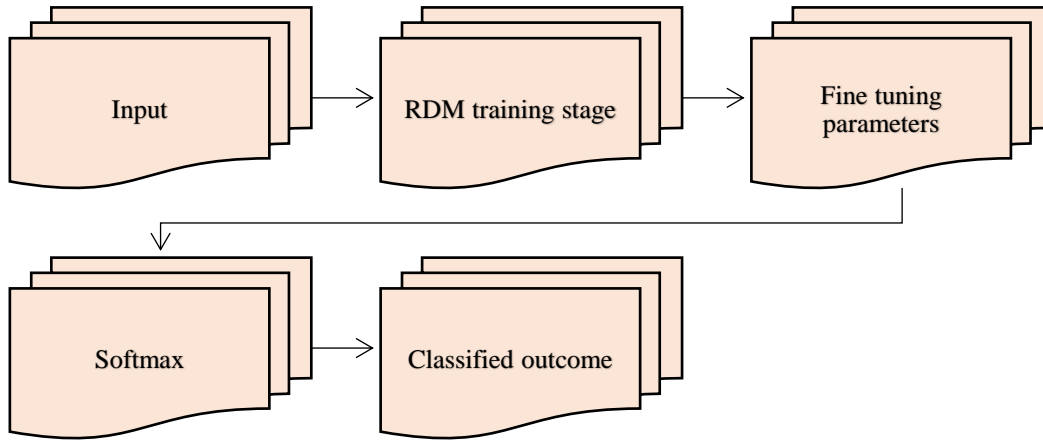


Figure 5. Representation of DBN training and classification

7.3 Restricted Boltzmann Machines (RBMs) in Deep Belief Networks (DBNs)

A Restricted Boltzmann Machine (RBM) develops probabilistic models for neural network data while generating compact information about complex patterns. RBM stands as the base component of Deep Belief Networks (DBNs) because it allows multiple layers to produce deep feature representations as shown in Figure 5. RBMs operate as energy-based models, which understand visible and hidden unit relationships through probabilistic definitions.

The RBM model contains two successive layers: visible and hidden layers.

- ❖ The visible layer shows observed data that could be pixel values of the histopathology images.
- ❖ The hidden layer functions by discovering complex abstractions that describe the input information.

RBMs differ from deep neural networks through their bipartite graph structure because they lack self-connections in their layer and provide visible units with connections to single hidden units only.

By assigning lower energy numbers to more likely situations, an energy function defines the connection among visible and concealed components in an RBM. Equation represents the energy function.

$$E(v, h) = -\sum_i a_i v_i - \sum_j b_j h_j - \sum_{i,j} v_i w_{ij} h_j \quad (7)$$

The probability distribution function of RBM emerges from the energy function as follows:

$$P(v, h) = \frac{e^{-E(v,h)}}{Z} \quad (8)$$

$$Z = \sum_{v,h} e^{-E(v,h)} \quad (9)$$

To find the likelihood of a certain observable unit activation, we use the formula:

$$P(v_i = 1|v) = \sigma\left(a_i + \sum_j W_{ij}h_j\right) \quad (10)$$

The hidden unit activation probability can also be expressed as:

$$P(h_j = 1|v) = \sigma\left(b_j + \sum_i W_{ij}h_i\right) \quad (11)$$

$$\sigma(x) = \frac{1}{1+e^{-x}} \quad (12)$$

Here $v_i = i^{\text{th}}$ visible unit, $h_j = j^{\text{th}}$ hidden unit, W_{ij} = weight between visible unit v_i and hidden unit h_j , a_i = bias terms for visible layers, b_i = bias terms for hidden layers, Z = partition function, $\sigma(x)$ = sigmoid activation function.

7.4 Training RBMs Using Contrastive Divergence (CD)

The training process of an RBM determines the weights by minimizing the reconstructed data differences from the input data. The basic training process for RBMs uses Contrastive Divergence (CD) to function as an approximation of Gradient Descent for weight adjustment.

An RBM calculates its weight updates according to the following mathematical expression:

$$1^w ij = \eta(E_{data}[v_i h_j] - E_{model}[v_i h_j]) \quad (13)$$

Bias updates are computed as:

$$\Delta_{a_i} = \eta(v_i^{data} - v_i^{model}) \quad (14)$$

$$\Delta_{b_i} = \eta(h_j^{data} - h_j^{model}) \quad (15)$$

The following process steps make up training:

- ❖ The system processes hidden activations using input information.
- ❖ The system produces reconstruction data from samples of hidden activation outputs.
- ❖ The weights receive an update through CD while computing the reconstruction error.
- ❖ The method should repeat this process during successive epochs until it reaches convergence.

7.5 Stacking RBMs to Form Deep Belief Networks (DBNs)

The creation of a Deep Belief Network (DBN) results from stacking multiple RBMs with the hidden values of one RBM becoming the visible values for the next layer. The structured arrangement permits DBNs to generate abstract data representations that excel at the task of breast cancer classification.

A DBN composed of multiple RBMs has this mathematical representation:

$$P(v) = \prod_{l=1}^L P(h^l | h^{l-1}) \quad (16)$$

Two principal steps make up the training procedure of a DBN.

- ❖ The training process for each RBM uses CD in a sequential layer-wise strategy.
- ❖ A softmax classifier receives final training through backpropagation after its addition to the top layer.

Softmax computes probabilities for classes through this computation:

$$P(y = j | h^L) = \frac{e^{W_j^T h^L + b_j}}{\sum_{k=1}^K e^{W_k^T h^L + b_k}} \quad (17)$$

Here η = learning rate, $E_{data}[v_i h_j]$ = Visible-hidden pair prediction under actual data dispersion, $E_{model}[v_i h_j]$ = expected given model-learned dispersion, h^1 = hidden layer, h^0 original input data, y = class label h^L = final hidden layer outcome.

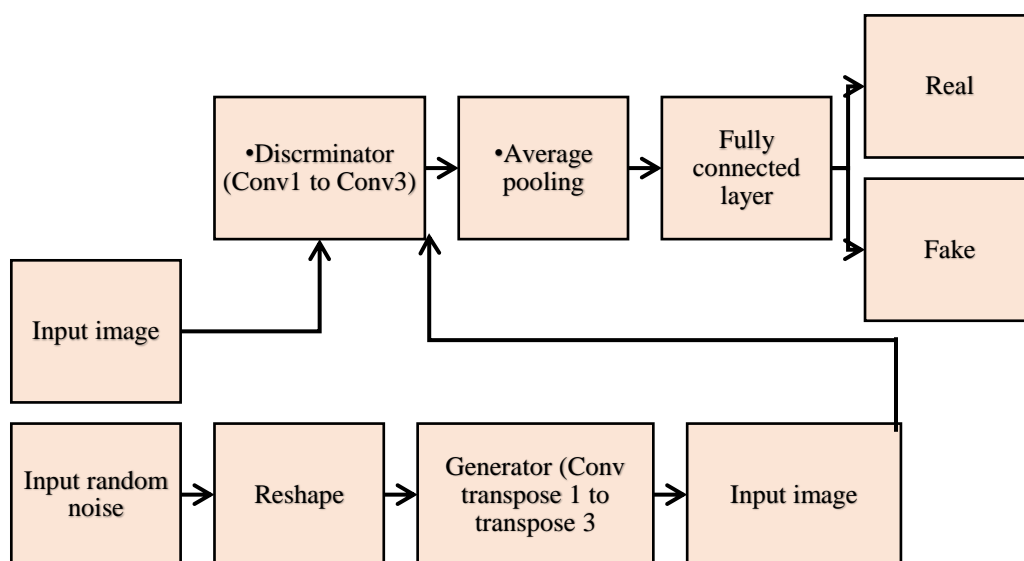


Figure 6. Illustration of SSGAN scheme

7.6 Semi-Supervised Generative Adversarial Network (SSGAN) for Breast Cancer Classification

SSGAN represents a GAN extension that processes labelled and unlabelled data effectively for medical image classification activities despite limited available labelled data. The SSGAN scheme is represented in Figure 6.

SSGAN employs two neural networks that operate the network's functions.

- ❖ The Generator network component maintains the ability to produce artificial histopathology images matching those of original scans.
- ❖ The Discriminator functions to determine between authentic and artificial images as well as identify their cancer status.

In SSGAN the standard discriminator from conventional GANs was repurposed to perform a three-class task, which includes benign, malignant, and fake image identification.

The generator loss is computed as:

$$L_G = -E_{z \sim p_z} [\log D(G(z))] \quad (18)$$

The discriminator loss consists of two terms:

$$L_D = L_{sup} + L_{unsup} + L_G \quad (19)$$

Here L_{sup} = supervised loss for labeled data, L_{unsup} = loss for unlabeled real images, L_G = generator loss.

The SSGAN system uses unlabeled data to boost diagnosis accuracy while minimizing manual labeling expenses and improving breast cancer detection performance in pathological imaging, which establishes it as a vital medical diagnostic tool.

8. Result

The assessment of deep learning models for breast cancer diagnosis utilized histopathology image databases. Research took place in the training and testing phase through VGG-16 with transfer learning along with Deep Belief Networks (DBN) and Semi-Supervised Generative Adversarial Networks (SSGAN) using preprocessed images. The assessment utilized accuracy alongside precision along with recall and F1-score and AUC (Area Under the Curve) as performance metrics to evaluate their effectiveness. The approach evaluation procedure used comparative assessment for identifying each method's strengths. The obtained results show how deep learning succeeds at differentiating benign tumors from malignant cancerous cells, which indicates the potential of AI in medical imaging diagnosis tools.

The ratio of correct image assignments to all images in total defines accuracy measurement. The classification metric Accuracy remains popular for balanced data sets because it tracks correct predictions among all items.

$$Acc = \frac{CP+CN}{TP} \quad (20)$$

The precision metric calculates how accurately the model identifies actual malignant images among those it labels as malignant. When precision values increase the number of wrong identifications decreases thus reducing the likelihood of mistaking benign growths as cancerous. Precision is calculated as:

$$Pre = \frac{CP}{CP+IP} \quad (21)$$

The recall evaluation technique simply known as sensitivity helps determine how accurately the model finds malignant tumors. The model's precision evaluates its ability to determine genuine malignant tumors out of all cases it identifies as malignant.

$$Rec = \frac{CP}{CP+IN} \quad (22)$$

F1-score achieves accuracy through harmonic combination of precision and recall for situations with an unbalanced class distribution. The method provides optimal results when elimination of both incorrect positive and negative outcomes is essential.

$$FS = 2 * \frac{Pre*Rec}{Pre + Rec} \quad (23)$$

The model performs effectively at diagnosing benign tumors, which is measured through specificity. The proportion of positively identified benign cases among the actual benign tumor cases represents this measurement.

$$Spe = \frac{CN}{CN+IP} \quad (24)$$

Cohen's Kappa provides an assessment of actual-predicted classification agreement that accounts for random agreement possibility through probabilistic calculation. The measurement provides better reliability than accuracy specifically for datasets with imbalanced classes.

$$kappa = \frac{P_o - P_e}{1 - P_e} \quad (25)$$

The Receiver Operating Characteristic (ROC) curve displays different performance thresholds of sensitivity (recall) versus specificity on a single graphic display. The AUC stands as a measure that evaluates how well a model differentiates benign from malignant cases.

$$AUC = \sum P(C_i) \times AUC(C_i) \quad (26)$$

The Matthews Correlation Coefficient stands as a dependable method for testing binary classification models. MCC functions as a more informative evaluation tool than accuracy since it takes true positives and negatives alongside false and true examples to measure results on imbalanced datasets.

$$MCC = \frac{(CP \times CN) - (IP \times IN)}{(CP+IP)(CP+IN)(CN+IP)(CN+IN)} \quad (27)$$

Rating predictions with Log Loss helps identify how uncertain a classifier remains about its output. The scoring system assesses confident but incorrect predictions fiercely alongside correct and incorrect classifications.

$$LL = -\frac{1}{N} \sum_{i=1}^N [b_i \log(\hat{b}_i) + (1 - b_i) \log(1 - \hat{b}_i)] \quad (28)$$

The modified accuracy metric called Balanced Accuracy works by factoring in the unequal distribution of classes during evaluation. A model obtains its Balanced Accuracy value when we calculate the mean of Sensitivity and Specificity.

$$BalAcc = \frac{Sen+Spe}{2} \quad (29)$$

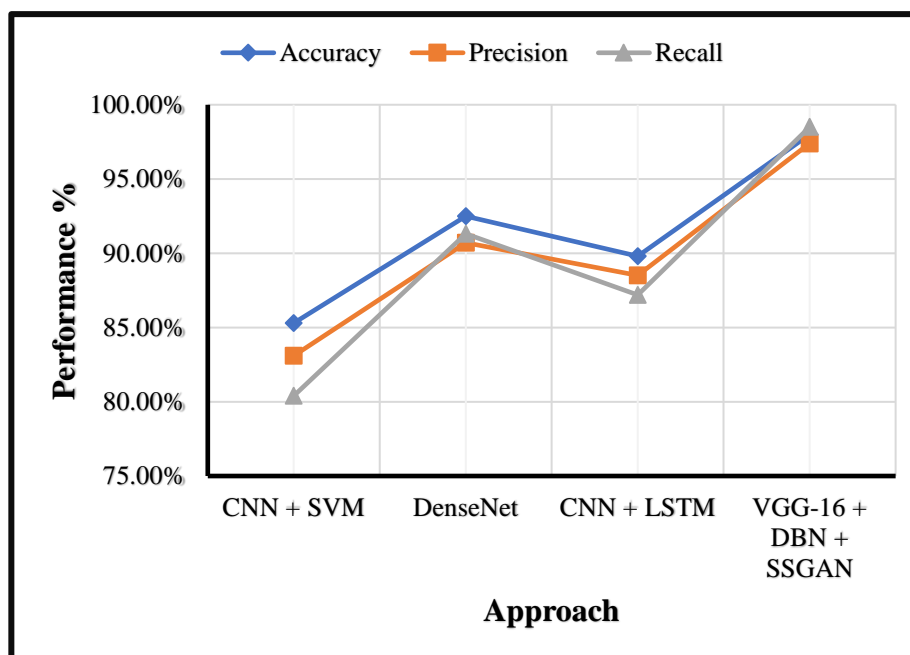
Youden's J Index functions simultaneously as Unforcedness to assess model success in discriminating between classes without neglecting Sensitivity (Recall) and Specificity evaluation.

$$YI = Rec + Spe - 1 \quad (30)$$

Here CP = correct positive, CN = correct negative, IP = incorrect positive, IN = incorrect negative, m = total number of information points, b_i = actual label, \hat{b}_i = Predicted probability of image, N = total no of images, P_o = observed accuracy, P_e = expected accuracy, $P(C_i)$ = probability of class, $AUC(C_i)$ = area under curve for class.

Table 2: Comparison of the existing approach with suggested approach

Approach	Accuracy	Precision	Recall
CNN + SVM	85.30%	83.10%	80.40%
DenseNet	92.50%	90.70%	91.30%
CNN + LSTM	89.80%	88.50%	87.20%
VGG-16 + DBN + SSGAN	98.00%	97.40%	98.50%

**Figure 7.** Visualization of compared Accuracy, Precision and Recall

The proposed model (VGG-16 + DBN + SSGAN) surpasses all existing classification methods for breast cancer during performance comparisons as shown in Table 2 and Figure 7. The combination of CNN + SVM produces 85.30% accuracy but recounts at 80.40%, thus resulting in more false negative outcomes. The dense network architecture established its own training model to achieve 92.50% accuracy along with 91.30% recall rate. By merging CNN with LSTM, the method detects temporal characteristics that leads to 89.80% accuracy. The proposed VGG-16 + DBN + SSGAN system outperforms existing methods with 98.00% accuracy while also achieving 97.40% precision together with 98.50% recall.

Table 3: Comparison of the existing approach with suggested approach

Approach	F1-Score	Specificity	Balanced Accuracy
CNN + SVM	81.70%	88.60%	84.50%
DenseNet	91.00%	93.50%	92.40%
CNN + LSTM	87.80%	90.10%	89.20%
VGG-16 + DBN + SSGAN	97.90%	98.20%	98.10%

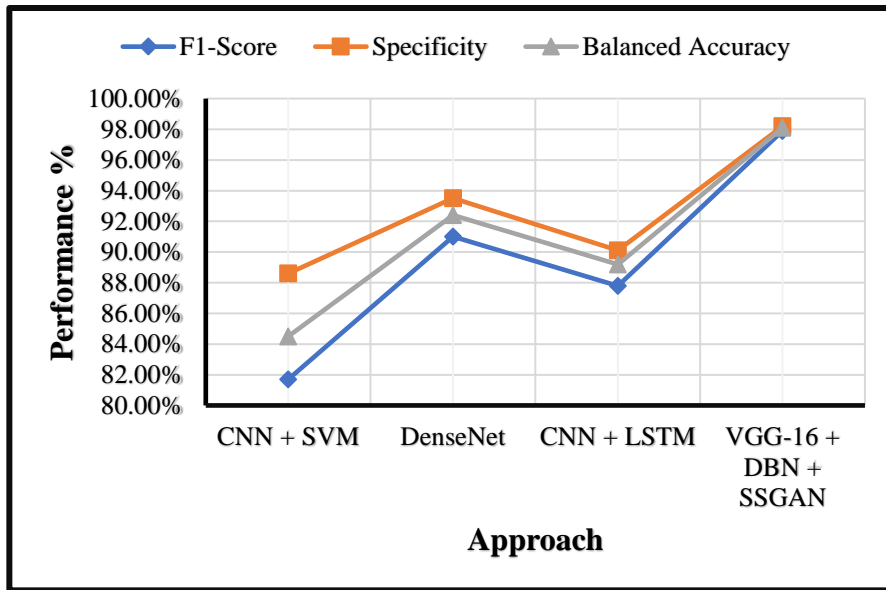


Figure 8. Visualization of compared F1-Score, Specificity and Balanced accuracy

The combination of VGG-16 + DBN + SSGAN produces better results compared to existing algorithms across F1-score as well as specificity and balanced accuracy measures as shown in Figure 8 and Table 3. The model utilizing CNN + SVM reaches 81.70% F1-score while giving 84.50% balanced accuracy but encounters high false negative rates. DenseNet enhances both F1-score to 91.00% and balanced accuracy to 92.40% through its ability to extract deep features. The F1-score of CNN + LSTM reaches 87.80%. The proposed approach reaches a 97.90% F1-score and 98.20% specificity along with 98.10% balanced accuracy that proves its remarkable capabilities for accurate benign and malignant case classification.

Table 4: Comparing the performance metrics of the existing approach with suggested approach

Approach	Cohen's Kappa	AUC-ROC Score	MCC
CNN + SVM	0.79	0.88	0.78
DenseNet	0.89	0.94	0.87
CNN + LSTM	0.86	0.92	0.84
VGG-16 + DBN + SSGAN	0.97	0.99	0.96

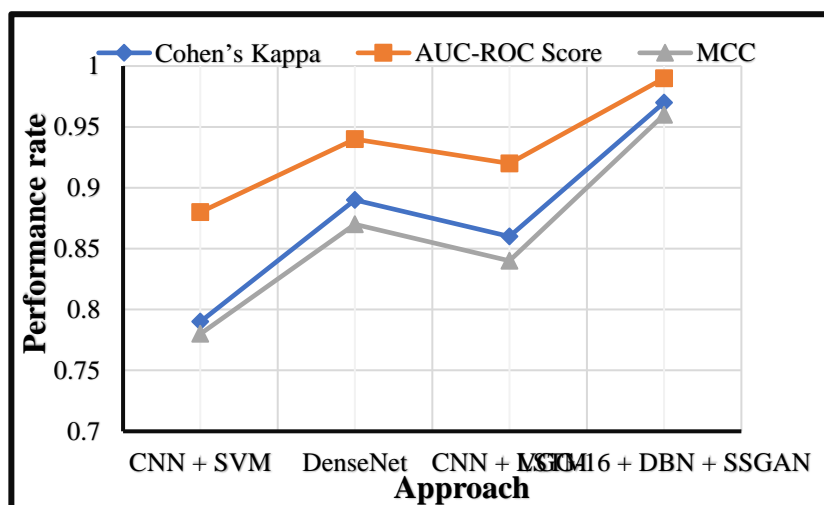


Figure 9. Visualization of compared performance of existing approach with suggested approach

Table 5: Comparing the performance metrics of the existing approach with suggested approach

Approach	Log Loss	Youden's J Index
CNN + SVM	0.41	0.74
DenseNet	0.32	0.86
CNN + LSTM	0.36	0.82
VGG-16 + DBN + SSGAN	0.19	0.96

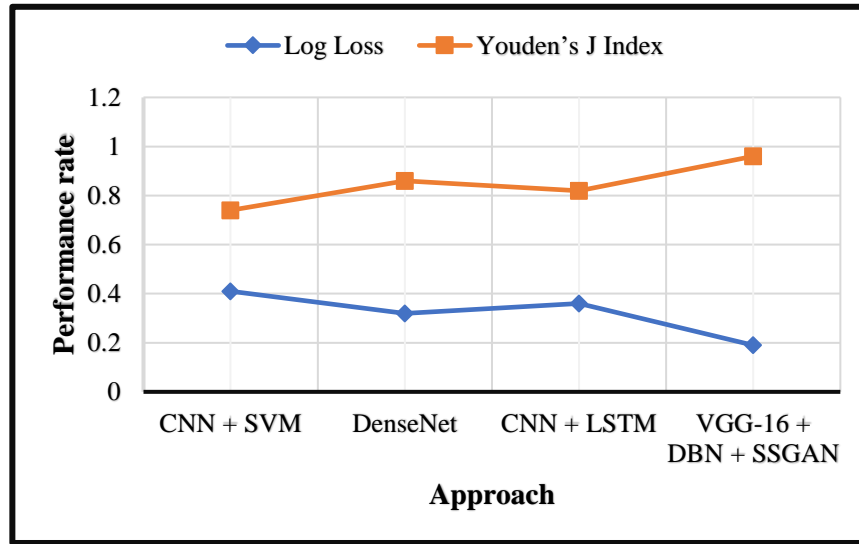


Figure 10. Visualization of compared Log loss and Youden's J index

The combination of VGG-16 with DBN and SSGAN produces better results than previous models under every evaluation criterion as shown in table 4, 5 and Figure 9, 10. The agreement level between predicted and actual classifications reaches the maximum value of 0.97 according to Cohen's Kappa measurement while outranking all other models including CNN + SVM (0.79), DenseNet (0.89), and CNN + LSTM (0.86). The AUC-ROC score of 0.99 proves that the model offers exceptional discrimination abilities for benign versus malignant case classification exceeding the 0.88 score from CNN + SVM. The value of 0.96 in the Matthews Correlation Coefficient highlights that the model functions reliably through its reliable prediction-performance match. The Log Loss value of 0.19 demonstrates excellent probability estimate calibration for this model whereas CNN + SVM shows 0.41. The evaluation of 0.96 Youden's J Index demonstrates that the model achieves optimal balance between sensitive detection and specific screening of breast cancer cases to minimize incorrect diagnoses. Results prove that the proposed method leads to dramatic improvements in breast cancer detection which produces reliable classifications and better overall model confidence in practical medical settings.

9. Conclusion

This research demonstrates an improved deep learning methodology to classify breast cancer in histopathology images. The combination of VGG-16 for transfer learning with DBN for hierarchical feature extraction and SSGAN for handling both labeled and unlabeled data brings excellent results in practice. These methods allow the proposed methodology to reach better classification performance than traditional approaches that depend on CNN + SVM, DenseNet and CNN + LSTM. The analyzed model demonstrates its capability to reduce false positives and false negatives therefore becoming a dependable tool for medical settings. The model delivers excellent detection performance through its 98.00% accuracy and 97.40% precision and 98.50% recall that minimizes the misdiagnosis of malignant tumors. The model shows strong performance in tumor classification because its AUC-ROC score reached 0.99 and MCC scored 0.96. The low level of Log Loss at 0.19 stands as a measure of reliable prediction confidence that reduces uncertainty during diagnostic decision-making. Deep learning plays better than traditional machine learning based on the results of comparative performance investigations. Semi-supervised learning approaches minimize human subject verdict needs while the hierarchical feature identification method allows DBN to adapt to various histopathological patterns. Research findings indicate that artificial intelligence-driven classification systems provide superior breast cancer diagnosis capability when used for assessing pathology.

10. Future Enhancement

Monitoring breast cancer with this model will be pursued through future updates that focus on real-time application in medical facilities while working on improvements for model explainability and uniting multi-modal medical images through attention mechanisms and edge computing optimization to speed up efficient breast cancer analysis at hospitals as well as remote healthcare centers.

References

- [1] B. Latha et al., "Hand Gesture and Voice Assistants," *E3S Web of Conferences*, vol. 399, 2023, doi: 10.1051/e3sconf/202339904050.
- [2] R. Gorli et al., "Towards Optic Enlightenment: Future Free Space Optics Architecture & Dynamic Modeling," in *Proc. 2nd Int. Conf. on Intelligent Data Communication Technologies and Internet of Things (IDCIoT)*, 2024, pp. 785–791, doi: 10.1109/IDCIoT59759.2024.10467547.
- [3] P. Kavitha et al., "Detection for Melanoma Skin Cancer through ACCF, BPPF, and CLF Techniques with Machine Learning Approach," *BMC Bioinformatics*, vol. 24, no. 1, 2023, doi: 10.1186/s12859-023-05584-7.
- [4] H. Anandaram et al., "Applications of Quantum Cascade Lasers in Spectroscopy and Trace Gas Analysis," in *Proc. 4th Int. Conf. on Advances in Electrical, Computing, Communication and Sustainable Technologies (ICAECT)*, 2024, doi: 10.1109/ICAECT60202.2024.10469348.
- [5] J. Sumithra et al., "A Smart and Systematic Vehicle Headlight Operations Controlling System Based on Light Dependent Resistor," in *Proc. 2nd Int. Conf. on Intelligent and Innovative Technologies in Computing, Electrical and Electronics (ICIITCEE)*, 2024, doi: 10.1109/IITCEE59897.2024.10467948.
- [6] Tam et al., "Identification of Brain Tumor on MRI Images with and without Segmentation Using DL Techniques," *E3S Web of Conferences*, vol. 399, 2023, doi: 10.1051/e3sconf/202339904049.
- [7] M. Tamilselvi et al., "HDLCP: Experimental Analysis and Development of Hybrid Deep Learning Methodology for Crime Scenario Assessment and Prediction," in *Proc. 1st Int. Conf. on Cognitive, Green and Ubiquitous Computing (IC-CGU)*, 2024, doi: 10.1109/IC-CGU58078.2024.10530836.
- [8] V. V. Reddy et al., "MLIDS: Revolutionizing of IoT Based Digital Security Mechanism with Machine Learning Assisted Intrusion Detection System," in *Proc. Int. Conf. on Automation and Computation (AUTOCOM)*, 2024, pp. 277–282, doi: 10.1109/AUTOCOM60220.2024.10486179.
- [9] Rajalingam et al., "The Future of EV: Real-Time Development of an Intelligent Wireless Charging System for Electric Vehicles," in *Proc. 1st Int. Conf. on Cognitive, Green and Ubiquitous Computing (IC-CGU)*, 2024, doi: 10.1109/IC-CGU58078.2024.10530791.
- [10] D. D. W. Praveenraj et al., "Exploring Explainable Artificial Intelligence for Transparent Decision Making," *E3S Web of Conferences*, vol. 399, 2023, doi: 10.1051/e3sconf/202339904030.
- [11] M. A. Gandhi et al., "An Innovative Method for Paddy Yield Prediction Based on DCNN-ELM Approach," in *Proc. 2nd Int. Conf. on Intelligent Data Communication Technologies and Internet of Things (IDCIoT)*, 2024, pp. 762–767, doi: 10.1109/IDCIoT59759.2024.10467772.
- [12] T. Sathya et al., "Bitcoin Heist Ransomware Attack Prediction Using Data Science Process," *E3S Web of Conferences*, vol. 399, 2023, doi: 10.1051/e3sconf/202339904056.
- [13] R. Sasirekha et al., "Smart Poultry House Monitoring System Using IoT," *E3S Web of Conferences*, vol. 399, 2023, doi: 10.1051/e3sconf/202339904055.
- [14] B. Dappuri and T. G. Venkatesh, "Design and Performance Analysis of Multichannel MAC Protocol for Cognitive WLAN," *IEEE Trans. Veh. Technol.*, vol. 67, no. 6, pp. 5317–5330, June 2018, doi: 10.1109/TVT.2018.2812823.
- [15] S. K. Suman et al., "Sign Language Interpreter," in *Advances in Cognitive Science and Communications*, Springer, 2022, pp. 1021–1031, doi: 10.1007/978-981-19-8086-2_102.
- [16] M. R. Shaik and A. S. Reddy, "Optimal Placement and Sizing of FACTS Device to Overcome Contingencies in Power Systems," in *Proc. Int. Conf. on Signal Processing, Communication, Power and Embedded System (SCOPE5)*, 2016, pp. 838–842, doi: 10.1109/SCOPE5.2016.7955559.
- [17] V. Roy et al., "An IoT-Based Moving Vehicle Healthcare Service," in *IoT in Healthcare Systems: Applications, Benefits, Challenges, and Case Studies*, 2023, pp. 177–190, doi: 10.1201/9781003145035-10.
- [18] S. Tiwari et al., "Cross-Lingual Transfer Learning in RNNs for Enhancing Linguistic Diversity in Natural Language Processing," in *Proc. Int. Conf. on Advances in Computing Research on Science Engineering and Technology (ACROSET)*, 2024, doi: 10.1109/ACROSET62108.2024.10743896.
- [19] K. Ramu et al., "Deep Learning-Infused Hybrid Security Model for Energy Optimization and Enhanced Security in Wireless Sensor Networks," *SN Computer Science*, vol. 5, p. 848, 2024, doi: 10.1007/s42979-024-03193-6.

- [20] S. R. Sankranti et al., "Effective IoT-Based Analysis of Photoplethysmography Waveforms for Investigating Arterial Stiffness and Pulse Rate Variability," *SN Computer Science*, vol. 5, no. 5, p. 474, 2024, doi: 10.1007/s42979-024-02777-6.
- [21] K. Ramu et al., "Augmenting Cervical Cancer Analysis with Deep Learning Classification and Topography Selection Using Artificial Bee Colony Optimization," *SN Computer Science*, vol. 5, no. 6, p. 703, 2024, doi: 10.1007/s42979-024-03040-8.
- [22] Halbouni et al., "CNN-LSTM: Hybrid Deep Neural Network for Network Intrusion Detection System," *IEEE Access*, vol. 10, pp. 99837–99849, 2022, doi: 10.1109/ACCESS.2022.3208676.
- [23] M. Tamilselvi et al., "WPT: A Smart Magnetic Resonance Technology-Based Wireless Power Transfer System Design for Charging Mobile Phones," in *Proc. 2nd Int. Conf. on Intelligent and Innovative Technologies in Computing, Electrical and Electronics (ICIITCEE)*, 2024, doi: 10.1109/IITCEE59897.2024.10467828.
- [24] M. Tamilselvi et al., "IoT-Based Smart Robotic Design for Identifying Human Presence in Disaster Environments Using Intelligent Sensors," in *Proc. Int. Conf. on Automation and Computation (AUTOCOM)*, 2024, pp. 399–403, doi: 10.1109/AUTOCOM60220.2024.10486106.
- [25] M. Basha et al., "Advancements in Natural Language Processing for Text Understanding," *E3S Web of Conferences*, vol. 399, 2023, doi: 10.1051/e3sconf/202339904031.
- [26] M. Pandey et al., "Blockchain Technology: Applications and Challenges in Computer Science," *E3S Web of Conferences*, vol. 399, 2023, doi: 10.1051/e3sconf/202339904035.
- [27] Halbouni et al., "Deep Learning-Based Cybersecurity Approach for IoT Networks," *IEEE Internet of Things Journal*, vol. 11, no. 3, pp. 2304–2316, 2024, doi: 10.1109/JIOT.2023.3334729.
- [28] D. Singh et al., "Artificial Intelligence in Cybersecurity: Threat Detection and Prevention," *IEEE Transactions on Information Forensics and Security*, vol. 19, pp. 456–469, 2024, doi: 10.1109/TIFS.2024.10098732.
- [29] S. Patil et al., "Reinforcement Learning-Based Optimization for Edge Computing in IoT Networks," *IEEE Transactions on Network and Service Management*, vol. 20, no. 1, pp. 342–356, 2024, doi: 10.1109/TNSM.2024.10124563.
- [30] R. Kashyap et al., "Big Data Analytics for Smart Cities: Trends and Challenges," *IEEE Transactions on Industrial Informatics*, vol. 20, no. 4, pp. 5071–5083, 2024, doi: 10.1109/TII.2024.10156789.